Analytical and experimental procedure for in situ stress measurements in prestressed concrete structures

Davide Messina[1], Chiara Galatà[1], Vincenzo D. Venturi[2], Antonino Recupero[1], Edoardo Proverbio[1]

1) Department of Engineering, University of Messina, Messina, Italy

2) Sidercemsrl, Misterbianco (CT), Italy

Abstract

A comprehensive understanding of in-situ stresses in prestressed concrete structures is essential for assessing their reliability. Special care must be given to deteriorated or corroded prestressed elements when determining their load-bearing capacity or designing retrofitting solutions. In prestressed components, such as beams, the stress distribution can vary along the span and height due to bending, shear, or eccentric prestressing, with variations depending on the distance from the section's centroid. Current methods for stress investigation in concrete structures include the flat jack method, portion removal method, and direct and indirect core-drilling techniques. These evaluations are subject to various influencing factors and uncertainties. An extensive experimental study has led to the development of a robust analytical framework for an enhanced incremental core-drilling method.

1 Introduction

A significant proportion of existing bridges within the European road and rail networks were constructed using Prestressed Concrete (PC), particularly with post-tensioned (PT) tendons. This preference stems from the superior performance of PC in terms of cracking resistance and deformability compared to Reinforced Concrete (RC), as well as its lower cost relative to steel structures, especially during the second half of the 20th century.

However, this structural typology may present deficiencies in terms of safety and load capacity primarily due to aging and/or prestress losses. Prestressing in concrete serves to mitigate the detrimental effects of cracking, thereby enhancing the protection of embedded reinforcements against corrosion. A reduction in the prestressing level corresponds to a decreased safety margin with respect to structural durability and long-term deterioration [1].

In response to these challenges, the Italian Guidelines for the Risk Classification and Safety Assessment of Existing Bridges [2] propose a systematic methodology to determine the appropriate level of attention for each bridge, based on its strategic importance and the extent of observed defects. In particular, PC bridge decks require precise testing to evaluate residual prestressing stress after long-term losses, as this has a direct impact on serviceability performance. PT tendons, in particular, are vulnerable to corrosion risks if voids are present within their ducts—an issue exacerbated in aggressive environmental conditions.

Numerous studies in the literature [3–6] emphasize the importance of in-situ measurement of prestressing stress to understand unexpected losses caused by factors such as relaxation, shrinkage, creep, or aggressive environments. Specifically, this paper proposes a method for conducting prestress release tests on prestressed concrete elements using concrete portion removal tests, which are currently among the most widely used semi-destructive methods. A common test in this context is core drilling, where strain is measured both before and after coring the concrete. This method involves positioning at least three strain gauges in different orientations on the external surface area around the core to accurately capture strain variations before and after the coring process [3].

The authors instead suggest placing at least three strain gauges on the exterior of the core, following a procedure already used in metallurgy, this latter case (known as *hole drilling*) allows the continuous measurement of the strain during the coring, differently from the former (known as *instrumented core extraction*) which allows the initial and the final measurements only [7]. The measured strains are directly related to the principal stresses which correspond to the concrete stress generated by the prestressing if the test is carried out in a null shear section and in the fiber of the centroid.

The conversion from strain to stress requires a strong assumption: that the concrete behaves as a homogeneous, isotropic, and linearly elastic material. Under this assumption, two mechanical parameters are necessary: Young's modulus and Poisson's ratio. While the latter exhibits only modest variations from a nominal reference value, the former depends on the concrete's strength, and any erroneous estimation can lead to significant errors in assessing the stress state.

This methodology has been applied to two case studies to obtain information about the actual prestressing stress after losses due to instantaneous and low reological phenomena. With the aim to contribute to the understanding of the limits and potentialities of the in-situ measurements of the prestressing stress, the results of the second case study have been compared and discussed to those obtained from a numerical analysis of the deck via a Finite Element (FE) analysis through the calculation code SAP 2000 [8].

2 Case study no. 1: Ritiro Viaduct

2.1 Description of the structure

The "Ritiro" viaduct is an infrastructure of the A20 Messina-Palermo highway, located between the Messina-Boccetta Gate and the Villafranca Tirrena Gate, originally built at the end of the 1960s and partially rebuilt between 2015 and 2024. The original PC deck consisted of two independent carriageways, respectively 924,10 m long for the carriageway towards Palermo, and 866,77 m for the one towards Messina. The former consisted of one special span of 44,30 m, 15 ordinary spans of 45,00 m, 5 short ordinary spans of 34,25 m, and one special span of 33,55 m, for a total of 21 piers and two abutments; the latter consisted of 17 ordinary spans of 45,00 m; 2 short ordinary spans of 34,25 m, and one special span of 33,55 m, for a total of 19 RC piers and two RC abutments. Both carriageways had a curved planimetric layout in the central part and a straight one at the ends, while the altitude profile showed different levels with the way to Palermo lower than the one to Messina. Due to deterioration over time and an increase in traffic, the Administration in 2014 decided to replace the deck with a steel-concrete grillage and to strengthen piers and abutments. An overview of the original Ritiro and Giostra Viaducts is shown in Fig. 1.

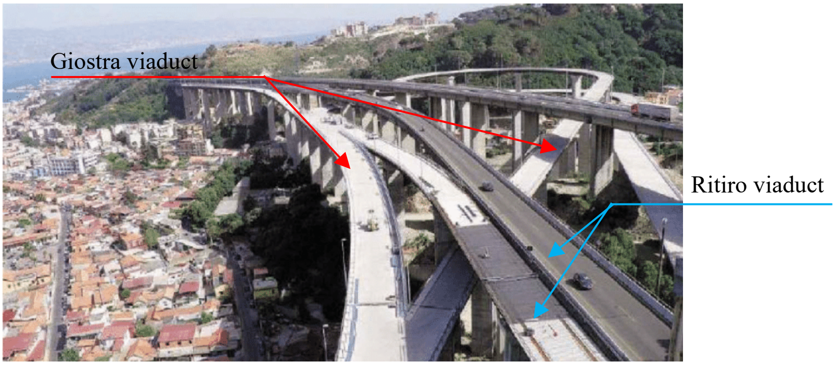

Fig. 1 - View of "Ritiro" viaduct and "Giostra" viaduct.

Each span was made up of a simply supported grillage of 4 PT girders and a variable number of RC diaphragms. The end diaphragms were entirely cast in place, instead those in the span were made using prefabricated elements made integral with the deck by casting sutures in place and subsequent transverse prestressing. There was no slab cast on site and the road support surface consisted of the upper bulb of the beams, having a thickness of 22 cm; the beams were made integral with each other by means of a longitudinal joint with reinforced concrete cast in situ, about 50 cm wide. The carriageway had a width of about 11,00 m. The end beams presented an upper nib of half joint as Gerber Saddle type (the beams passed from a height of 2.70 m to a height of 1.31 m). The bearings of the beams were in reinforced rubber.

The central beams were equipped with 5 parabolic tendons of 40 wires with a 7 mm diameter (40ϕ7), while the edge beams have 6 parabolic tendons of 30 wires with a 7 mm diameter (30ϕ7). This configuration optimizes load distribution based on the position and structural role of the beams.

The piers are made of RC with a height ranging from 14 m to approximately 63 m and a hollow rectangular cross-section; the plan dimension in the transverse direction to the longitudinal axis of the viaduct was constant and equal to 6,40 m, while the other dimension in the longitudinal direction was variable with the height of the pile, with a minimum of 2,40 m.

2.2 Experimental measurements

During the demolition of the previous deck, a side girder of an ordinary span was isolated from the grillage, leant on the ground, and put at the authors' disposal to conduct an in-situ test to extimate the residual prestressing. In detail, a core drilling test was conducted through both external (hole drilling) and internal (instrumented core extraction) strain measurements. The former involved the application of five external resistive strain gauges (named E4, E5, E6, E7, E8) and a triplet of internal strain gauges (named a, b, c) that measure the strains resulting from the modification of the stress state around the hole created through the coring (see Fig. 2). Actually, three strain gauges would be enough to define the principal strains and stresses, therefore the other two external have been used as check measures.

The test was conducted at a distance of about 7 m from the bearing and a height of about 80 cm from the upper bulb. During the test, the deformation values (in microstrain) of the 5 external strain gauges and the 3 internal strain gauges were recorded as a function of the coring depth, as shown in Fig. 3.

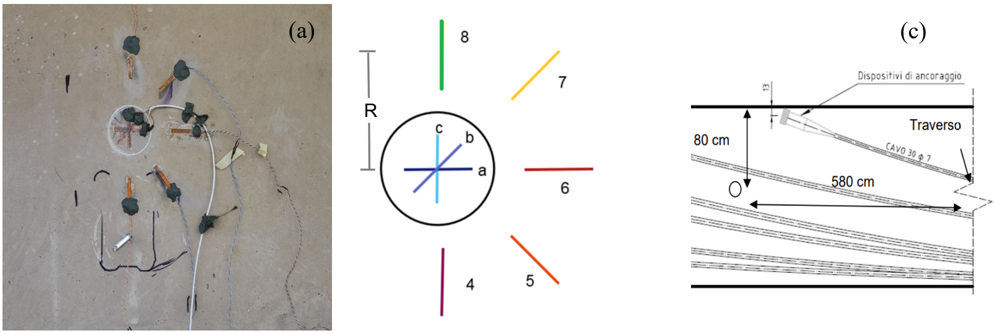

Fig. 2 - Layout of the strain gauges: picture in situ (a), sketch (b), core position in the beam (c).

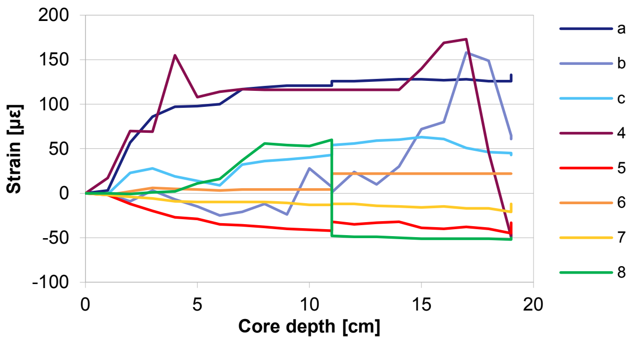

Fig. 3 - Plot of the strain gauge record.

2.3 Interpretation of results

2.3.1 Hole drilling method

Assuming an elastic behavior of the material, the previous strains can be correlated to the in situ principal stresses σ_1 and σ_2 (which correspond to the maximum and the minimum stress, respectively) acting before drilling, and the angle with the horizontal direction α, as follows:

$$\sigma_1 = \frac{\varepsilon_1+\varepsilon_3}{4A} - \frac{1}{4B}\sqrt{(\varepsilon_3-\varepsilon_1)^2+(\varepsilon_3+\varepsilon_1-2\varepsilon_2)^2} \quad (1)$$

$$\sigma_2 = \frac{\varepsilon_1+\varepsilon_3}{4A} + \frac{1}{4B}\sqrt{(\varepsilon_3-\varepsilon_1)^2+(\varepsilon_3+\varepsilon_1-2\varepsilon_2)^2} \tag{2}$$

$$\tan 2\alpha = \frac{\varepsilon 1-2\varepsilon 2+\varepsilon 3}{\varepsilon 1-\varepsilon 2} \tag{3}$$

Where the coefficients A, and B are calculated in the function of the coefficient $r = R_0/R$, with $R_0 = 50$ mm (core radius), and $R = 130$ mm (distance from the center of the core to the midpoint of the strain gauge), and of the Young modulus $E = 33.148$ MPa (evaluated according to NTC 2018 starting from a medium cylindrical compressive strength $f_{cm} = 39{,}2$ MPa) and Poisson modulus $\nu = 0{,}2$ of the concrete.

$$A = -\frac{1+\nu}{2E}\left(\frac{1}{r^2}\right) \tag{4}$$

$$B = -\frac{1+\nu}{2E}\left[\left(\frac{4}{1+\nu}\right)\frac{1}{r^2}-\frac{3}{r^4}\right] \tag{5}$$

These parameters not only incorporate the elastic properties of the material under test but also reflect the severe attenuation of the released deformations relative to the relaxed stresses [9].

The results obtained through in situ measurements are: $\sigma_1 = 4{,}83$ MPa (compressive); $\sigma_2 = -0{,}07$ MPa (tensile); $\alpha = -15{,}5°$.

2.3.2 Instrumented core extraction

Regarding the internal strain gauges, the formulas found in the literature were applied in order to obtain the two principal stresses σ_1 and σ_2, and the angle of the principal direction α:

$$\sigma_{1,2} = E\left[\frac{(\varepsilon_a+\varepsilon_b+\varepsilon_c)}{3*(1-\nu)} \pm \frac{1}{1+\nu}\sqrt{\left(\varepsilon_a-\frac{(\varepsilon_a+\varepsilon_b+\varepsilon_c)}{3}\right)^2+\frac{(\varepsilon_c+\varepsilon_b)^2}{3}}\right] \tag{6}$$

$$tan(2\alpha) = \left(2\varepsilon_b-(\varepsilon_a+\varepsilon_c)\right)/(\varepsilon_a-\varepsilon_c) \tag{7}$$

The results obtained through in situ measurements are: $\sigma_1 = 4{,}79$ MPa (compressive), $\sigma_2 = 1{,}75$ MPa (compressive), $\alpha = -15{,}5°$; therefore, the results of the two methods are quite similar. It is worth specifying that σ_1 is the principal stress and not the longitudinal stress σ_x (see Eq. (8)), which is directly comparable to the theoretical one calculated with Navier's formula (where subscript *b* refers to box-girder) reported in Eq. (9):

$$\sigma_x = \frac{\sigma 1+\sigma 2}{2} + \frac{\sigma 1-\sigma 2}{2\ cos\alpha} \tag{8}$$

$$\sigma_N = \frac{N}{A_b} + \left(\frac{N*e}{I_b}\right)\cdot \mathrm{y} \tag{9}$$

Where σ_x is equal to 4,48 MPa, while σ_N, considering a prestress of the tendons after losses of 900 MPa, is equal to 6,08 MPa, hence no prestressing loss due to corrosion is expected. In addition, a segment of one tendon was extracted from the girder and no corrosion evidence was detected [10].

3 Case study no. 2: Vallone Marzo Viaduct

3.1 Description of the structure

The second case study examined concerns a PT pre-cast segmental box-girder bridge, forming part of the Messina-Palermo highway, near the municipality of Cefalù, known as "Vallone Marzo" viaduct. It was constructed in 1988 with a variable-depth box section continuous girder made up of two lateral spans 49,95 m long and one central span 99,9 m long, supported by two piers and two abutments, for a total bridge length of 149,84 m. The lateral and the central spans are composed of 17 and 33 precast PC segments respectively, made integral through PT harmonic steel tendons (composed of 12 strands with a diameter of 0.6" each) located in protective conducts injected with mortar. The top prestressing system consists of 56 tendons for each span, instead the bottom one consists of 16 and 26 tendons for lateral and central spans respectively. The prestressing layout can be observed in Fig. 4.

The girder segments are characterized by a single-cell box section with two webs, an upper slab and a lower counter slab; the upper slab is provided with 2 lateral cantilevers to accommodate the entire roadway, on which there are RC curbs, equipped with prefabricated guardrails. Specifically, the segments have an upper width of 11 m, a lower width of 5,40 m, a constant upper slab thickness of 0,26 m and a variable counter-slab thickness. Fig. 5 shows an overview of the viaduct, and a head-pier and a midspan cross sections.

A C50/60 and a C25/30 were adopted as design concrete classes for girder and piers/abutments respectively; moreover, from in-situ tests carried out on girder concrete, an average compressive strength f_{cm} of 58 MPa was detected. The harmonic steel used for tendons has an ultimate characteristic strength f_{ptk} of 1700 MPa from design draws.

The two piers are realized with a box girder section 5,40 x 5,00 m, with 50 cm thickness and heights 13 and 15 m based on a well foundation. The two abutments have a cantilever layout with 11 m width, 10 m long and 10,50 m height, based on well foundation too.

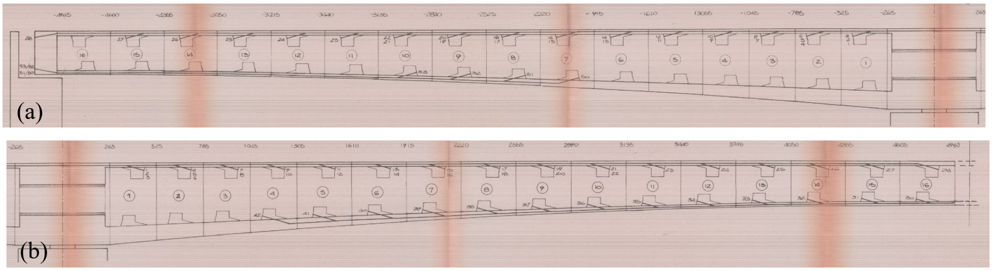

Fig. 4 - Prestressing tendons layout: abutment-pier (a); pier-midspan (b).

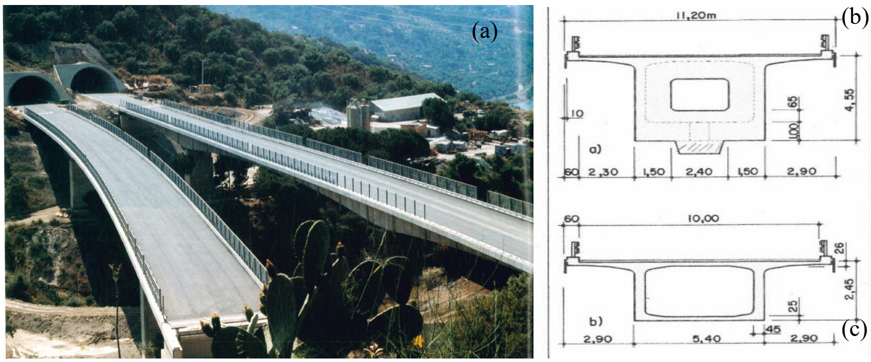

Fig. 5 - Vallone Marzo viaduct: overview (a); head-pier cross-section (b); midspan cross-section (c).

3.2 Stress release tests (in situ tests)

To estimate the value of residual prestress in the bridge deck, core drilling tests were carried out in situ on the concrete. The test consisted of the application of four external resistive strain gauges (E1, E2, E3, E4) properly bonded to the internal web surface of the prestressed concrete segment and a triplet of strain gauge rosettes on the base surface of the core (however measurements have not been taken into account because considered not reliable), in order to determine the strains resulting from the modification of the stress state around the hole made with a core drill, as shown in Fig. 6. The strains, assuming an elastic behaviour of the material, can be related to the in-situ stresses existing before the drilling. These tests were carried out in the central span of the viaduct, both in the direction of Palermo and in the direction of Messina, in segment no. 16, at a distance from the bottom slab of 1,22 m.

During the test, the strain values (in microepsilon) of the 4 external strain gauges were recorded as the time changed, measured in seconds, as shown in Fig. 7. Since strain gauges "d" and "g" are positioned in the same direction, only one strain gauge $\varepsilon_d = \varepsilon_g$ was taken into consideration, with the average strain value.

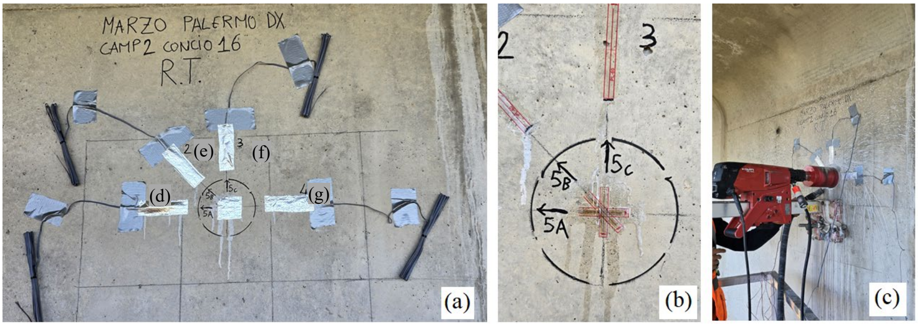

Fig. 6 - Strain gauge layout (a); detail of internal strain gauges (b); concrete coring (c).

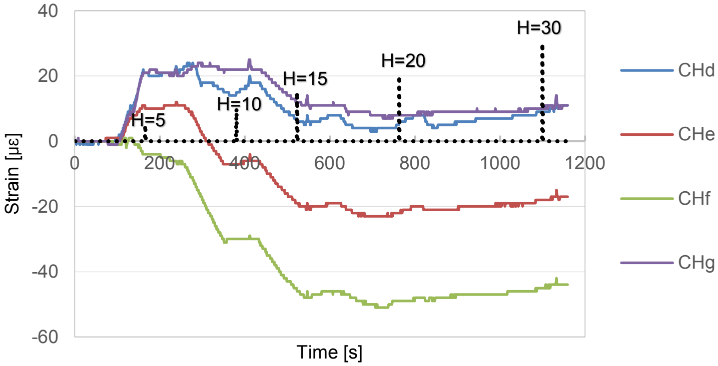

Fig. 7 - Plot of the strain gauge record; black dot lines represent the coring depth H expressed in cm.

The coefficients A, and B of the Eqq. (4), (5) are calculated as in the function of the coefficient $r = R_0/R$, with R_0 = 55 mm, and R = 130 mm, and E = 37.278 MPa (evaluated according to NTC 2018 starting from f_{cm} = 58 MPa) and ν = 0,2 of the concrete.

Finally, the principal stresses σ_1 and σ_2, as well as the inclination of the principal direction with respect to the horizontal α, were evaluated from the in-situ tests, using the expressions previously derived (Eqq. (1), (2), (3)). The results obtained through in situ measurements are: σ_1 = 3,51 MPa (compressive); σ_2 = 0,78 MPa (compressive); α = -2,08°.

3.3 FEM modeling

After evaluating the results obtained from the in-situ release test, a numerical analysis of the bridge was performed using the FE model developed in SAP2000 where only the bridge deck was considered, while the piers and abutments were replaced with specific constraints only. This approach simplifies the analysis still maintaining an accurate representation of the structural support conditions.

For the modeling, it is assumed that, given the elapsed time, the effects of the final static scheme consolidation have already been accounted for.

The deck was modelled as a beam element, with variable-height segments according to original design documents, as shown in Fig. 8. The prestress was applied by assigning equivalent forces and moments at the centroid of each deck segment to account for the eccentricity of the tendons and prestressing losses. In detail, shrinkage, creep, steel relaxation, friction, and anchorage slip have been considered, obtaining a loss factor β=1,45. Moreover, the self-weight and the superimposed loads were assigned, while the traffic load was neglected due to their absence during the execution of the tests.

A linear structural analysis was carried out with the evaluation of the internal forces, in particular the axial force N, the bending moment M and shear V forces acting along the bridge axis under the quasi-permanent load case, as reported in Fig. 9. Since the release test was performed in segment 16 of the central span, the internal forces are evaluated in the same section and are equal to: N= –38.122 kN, M= –13.669 kNm, V = 478 kN.

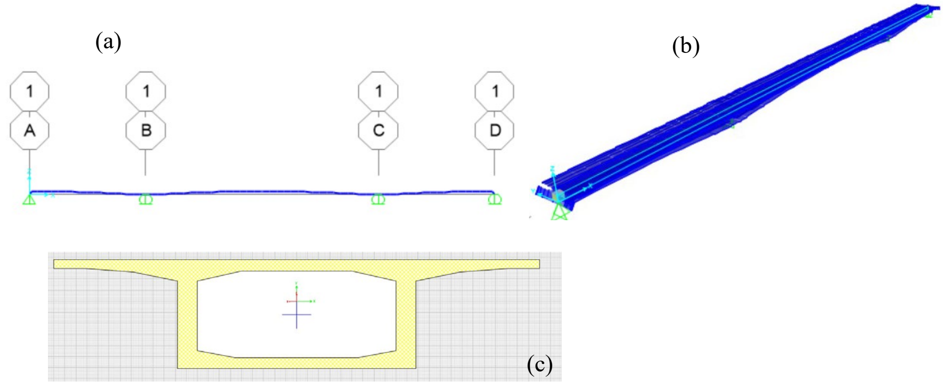

Fig. 8 - Model of the continuous girder (a), extruded overview (b), typical cross section (c).

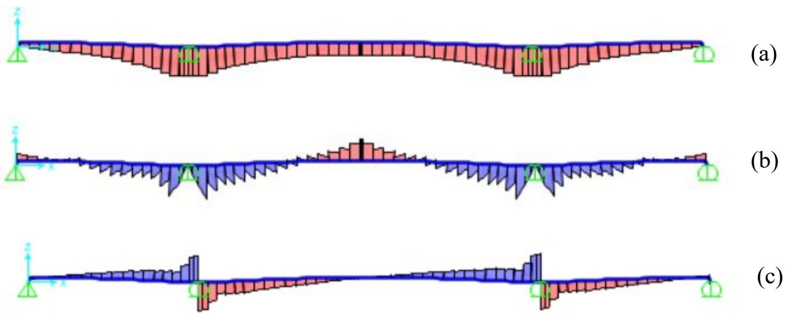

Fig. 9 - Axial force (a), bending moment (b), and shear (c) diagrams in quasi-permanent combination.

Finally, after calculating the applied stresses, the normal stresses σ were calculated using Navier's formula (see Eq. (9)) and the shear stresses τ were calculated using Jourawski's formula (subscript b refers to box-girder, w refers to the web):

$$\tau = \frac{V \cdot S_b}{I_b \cdot b_w} \tag{10}$$

The principal stresses σ_1 and σ_2 were then evaluated using the following relations:

$$\sigma_1 = \frac{1}{2}|\sigma_N| + \sqrt{\left(\frac{\sigma_N}{2}\right)^2 + \tau^2} \tag{11}$$

$$\sigma_2 = \frac{1}{2}|\sigma_N| - \sqrt{\left(\frac{\sigma_N}{2}\right)^2 + \tau^2} \tag{12}$$

The values of σ_1 and σ_2 are equal to 6,66 MPa and -0,002 MPa and the principal orientation angle α is equal to 0,9°. A comparison between the experimental and numerical results is reported in Table 1.

A comparison between theoretical and experimental results suggests a noticeable discrepancy, which may be a warning. However, due to the lack of precise data on the actual properties of the materials used – primarily the Young's modulus of the concrete, which is in a linear relationship with the stress – as well as details on the assembly phases, the authors were compelled to make certain assumptions. In fact, the discrepancy may be addressed also to a local phenomenon, therefore a more in-depth investigation in more points of the deck could clarify the reasons in the coming months.

Table 1 - Comparison between experimental and numerical results of Vallone Marzo viaduct.

	Experimental	Numerical
σ_1 (MPa)	3,51	6,66
σ_2 (MPa)	0,78	-0,002
α (°)	-2,08	1,10

4 Conclusions

In this study, a semi-destructive method was proposed to estimate prestressing stress which is an essential parameter for evaluating the structural health of a bridge, as well as an indirect indicator of cross-sectional reduction in prestressing tendons due to corrosion. The in-situ core drilling test provided valuable information on residual stress within the concrete. Two techniques, namely the “hole drilling” method and the “instrumented core extraction” method, were analyzed and applied to two distinct case studies.

The first case study involved a side beam from a decommissioned PT grillage deck, where a comparison was made between stresses obtained from external and internal strain gauge measurements and those calculated using Navier’s formula. In the second case study – focused on a box-girder deck, which requires greater attention due to its complexity – a FE model was also developed. The comparison between experimental results and numerical predictions revealed some discrepancies in the second case study. These are likely attributable to uncertainties in input data and potentially higher prestress losses than initially estimated. The observed discrepancies indicate that further calibration of the numerical model may be necessary, particularly in refining assumptions related to material properties and prestress loss estimation. Future work will address these additional considerations to better understand the source of the observed deviations.

References

[1] Messina D, Proverbio E. Effect of prestressing corrosion on failure in bridges. Structural Concrete 2023;24:227–38. https://doi.org/10.1002/suco.202200360.

[2] Italian Ministry of Infrastructures. Guidelines for classification and risk management, safety assessment, and structural health monitoring of existing bridges [Linee Guida per classificazione e gestione del rischio, valutazione della sicurezza e monitoraggio ponti esistenti] (in Italian). 2020.

[3] Azizinamini A, Keeler BJ, Rohde J, Mehrabi AB. Application of a New Nondestructive Evaluation Technique to a 25-Year-Old Prestressed Concrete Girder. PCI Journal 1996;41:82–95. https://doi.org/10.15554/pcij.05011996.82.95.

[4] Kraľovanec J, Moravčík M, Bujňáková P, Jošt J. Indirect determination of residual prestressing force in post-tensioned concrete beam. Materials 2021;14. https://doi.org/10.3390/MA14061338/MATERIALS_14_01338_PDF.PDF.

[5] Pessiki S, Kaczinski M, Wescott HH. Evaluation of effective prestress force in 28-year-old prestressed concrete bridge beams. PCI Journal 1996;41:78–89. https://doi.org/10.15554/PCIJ.11011996.78.89.

[6] Bagge N, Nilimaa J, Elfgren L. In-situ methods to determine residual prestress forces in concrete bridges. Eng Struct 2017;135:41–52. https://doi.org/10.1016/j.engstruct.2016.12.059.

[7] Proverbio E, Recupero A, Venturi V. Integrating destructive and non-destructive inspection techniques in evaluating tendon corrosion in posttensioned concrete beams. 3rd CACRCS Workshop, 2021, p. 263–266.

[8] Computers and Structures Inc. CSi analysis reference manual for SAP2000® 2016.

[9] P. V. Grant, J.D. Lord, P.S. Whitehead. Tech-Note TN-503. Measurement of Residual Stresses by the Hole-Drilling Strain Gage Method. 2010.

[10] Giglio M, Messina D, Recupero A, Proverbio E. Issues in estimating corrosion rate of steel wires for remaining service life prediction in post tensioned concrete structures. 4th CACRCS Workshop, Parma, Italy: 2023, p. 311–4.